Chapter 3

MATERIALS AND METHODOLOGY

This chapter outlines the experimental procedures for developing bio-HEAs and characterizing microstructural, mechanical, corrosion, wear, and in-vitro biocompatibility properties.

3.1 Materials selection for the development of HEAs

In the present study, the elemental powder titanium, niobium, zirconium, tantalum, chromium, iron, and cobalt are purchased from Alfa Aesar (U.K.), having a purity of 99.99 %. The BT-XRD (bench top XRD) test is carried out for confirmation of purity. A thorough review of existing literature carefully guided the selection of these specific elements to develop biocompatible HEAs. Thus, the chosen elements were strategically aligned with the overarching goal of formulating HEAs tailored for enhanced biocompatibility, marking a step toward addressing the needs of biomedical applications.

3.2 Methods of development of HEAs

HEAs composed of Ti, Nb, Ta, Zr, Cr, Fe, and Co with a nominal composition of Ti-$Co_{0.35}$-$Cr_{0.35}$-Nb-Zr, Ti-Nb-Ta-Cr-$Co_{0.2}$, and Ti-Nb-Ta-$Fe_{0.35}$-$Co_{0.35}$ (at. %) were synthesized using planetary high-energy ball milling (Synthano, India). Initially, all the powders were subjected to milling in a 125 mL tungsten carbide jar with 10 mm diameter tungsten carbide balls. During the milling process, the jar was rotated at a speed of 400 rpm in a counter-clockwise direction with a ball-to-powder weight ratio of 10:1. The schematic diagram for the milling process in high-energy ball milling is shown in Fig. 3.2. To prevent oxidation, the milling

operation was conducted within an argon environment. Additionally, to avoid overheating and unwanted phase changes, the process was stopped for 15 min after every 30 min of operation. Samples were extracted at various time intervals to analyze the impact of milling on the microstructure and phase evolution. To prepare a powder sample for the TEM analysis, small amount of powder milled for 50 h was dispersed in a vial containing methanol. The vial was then ultrasonicated for 30 min to ensure uniform distribution. The resulting sample was then drop-cast onto a copper grid coated with carbon and subsequently dried for 1 h under an infrared lamp prior to analysis.

To consolidate the 50 h alloyed powder, muffle furnace sintering (for Ti-$Co_{0.35}$-$Cr_{0.35}$-Nb-Zr HEA) and SPS (for Ti-Nb-Ta-Cr-$Co_{0.2}$, and Ti-Nb-Ta-$Fe_{0.35}$-$Co_{0.35}$ HEA) techniques were employed. For muffle furnace sintering, the 50 h alloyed Ti-$Co_{0.35}$-$Cr_{0.35}$-Nb-Zr HEA powder was consolidated into green pellets of diameter 15 mm with the help of a hydraulic press at a pressure of 720 MPa for 30 s (Fig. 3.2). These green pallets were vacuumed sealed (10^{-6} torr) and sintered at temperatures 750, 850 and 950 °C with a heating rate of 4 ℃ min^{-1} for 5 h. For the SPS process, the 50 h alloyed powders Ti-Nb-Ta-Cr-$Co_{0.2}$, and Ti-Nb-Ta-$Fe_{0.35}$-$Co_{0.35}$ HEA were heated at a rate of 100 ℃/min while maintaining a constant holding pressure of 50 MPa until it reached a temperature of 1000 °C. A vacuum environment of 10^{-6} torr was maintained throughout the process to prevent oxidation. For the sintering, cylindrical graphite die and punch were used. To facilitate the easy removal of the sample and punch, a graphite foil of thickness 0.2 mm was wrapped around the inner layer of the die. The resulting sintered samples had a diameter of ∼15 mm and a thickness of ∼8 mm. All the sintered samples' surfaces were grinded using emery papers and polished using diamond paste. For microstructure analysis, the polished samples were etched using Kroll's reagent (92 % H_2O, 6 % HNO_3, and 2 % HF). The schematic representation of the SPS HEAs synthesis is shown in Fig. 3.3, and the polished HEAs sample is shown in Fig. 3.4.

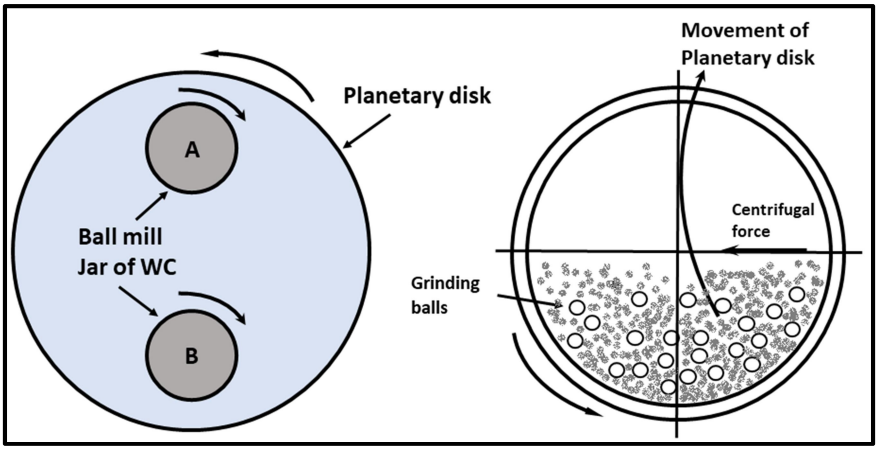

Fig. 3.1. Schematic diagram for the milling process in high-energy ball milling.

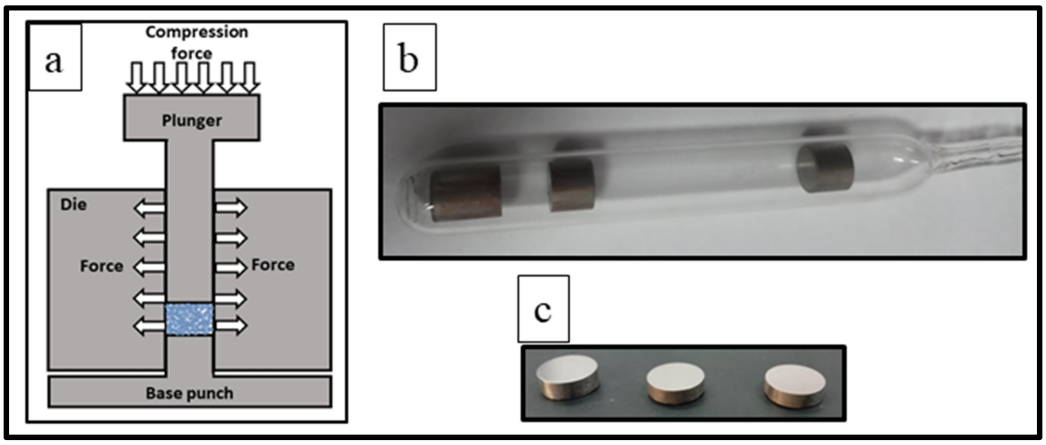

Fig. 3.2. (a) Schematic diagram for compaction of powder in die for muffle furnace sintering, (b) quartz tube sealing, and (c) muffle furnace sintered samples.

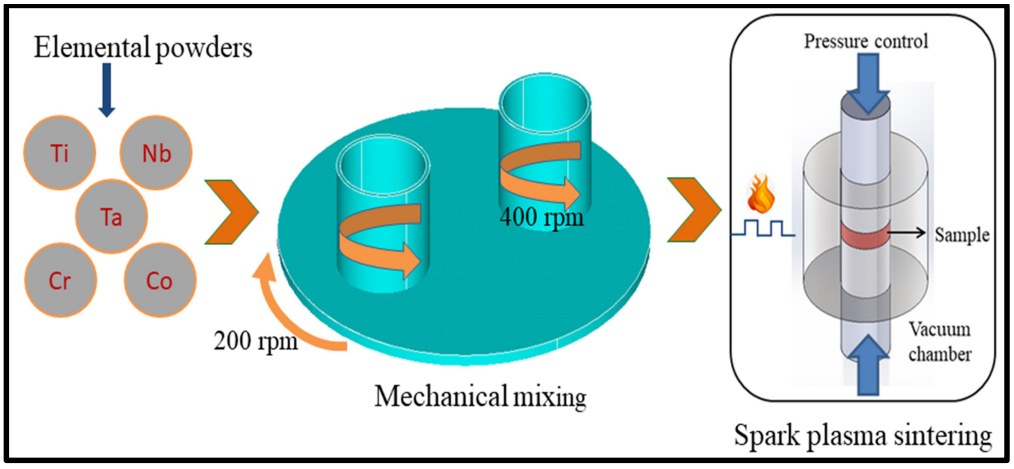

Fig. 3.3. Schematic representation of the synthesis of SPS HEAs.

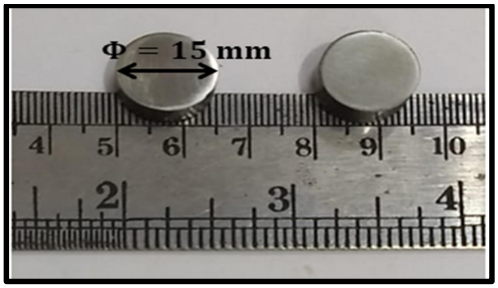

Fig. 3.4. Sintered HEAs polished samples (diameter = 15 mm and thickness = 8 mm).

3.3 Phase evaluations and microstructural characterizations of the HEAs

The structure, microstructure, and phase evolution of the alloyed and sintered samples were characterized using XRD (Rigaku Mini flex-600), TEM (TECNAI G2T20), and SEM (FEI Quanta 200F). XRD analysis was performed in the 2θ range of 20-90° and the peak pattern was analyzed using X'Pert Plus software (PANalytical). Chemical composition and elemental mapping of the alloyed and sintered samples were assessed using EDS coupled with field emission scanning electron microscopy (FE-SEM). For SEM and EDS analysis of the alloyed powder, the samples were coated with Au/Pd [(60/40) wt %] to improve the conductivity and contrast of the images. Thermal investigation of the 50 h milled powder was carried out using DSC (NETZSCH 404 F3) in a nitrogen environment with a flow rate of 25 mL/min and a heating rate of 10 °C/min for an operating temperature range of 25 to 1100 °C.

3.4 Mechanical properties testing

3.4.1 Density of the sintered HEAs

The sintered sample density was determined using Archimedes' principle (ASTM C 693) with the help of the calculated weight in air and water using an electronic weight balance with an accuracy of 10^{-4} grams. The theoretical density of the alloy is calculated using the

rule of the alloy mixture, Eq. (3.1). The samples relative density and porosity are computed using Eqs. (3.2 and 3.3), respectively.

$$\rho_t = \left(\frac{\sum c_i A_i}{\sum \frac{c_i A_i}{\rho_i}} \right) \tag{3.1}$$

$$Relative\ density\ (\%) = \left[\frac{\rho_s}{\rho_t} \right] \times 100 \tag{3.2}$$

$$Porosity = \left(1 - \frac{\rho_s}{\rho_t} \right) X\ 100\ \% \tag{3.3}$$

Where, ρ_t and ρ_s are, respectively, the theoretical density and calculated density of the sintered HEA sample.

3.4.2 Microhardness and Young's modulus of the sintered HEAs

The microhardness (*H*) and Young's modulus (*E*) were calculated employing an instrumented microhardness machine (MHT^3, Anton Paar). The indentation process involved the following testing parameters: a maximum applied load of 5000 mN, an approach speed of 80 μm/min, a retract speed of 16 μm/min, a loading rate of 10000 mN/min, and a holding period of 20 s. The Oliver-Pharr method [202] was employed to calculate the *H* and *E* values based on the loading and unloading curves. Six indentations were performed, and the resulting average values of hardness, indentation depth, and Young's modulus were reported. A Vickers hardness tester was also used to assess the sintered samples' bulk hardness (Leco LV248AT). A load of 300 gf was imposed on the sample for 10 sec. The microscope is used to observe the indentation left on the specimen's surface upon applying a load and to compute the average of the two diagonals of the indentation after the load removal. The Vickers hardness is determined based on the relationship between the applied load and the square millimetre area of the indentation (Fig. 3.5). The Vickers microhardness is calculated by using Eq. (3.4). The average Vickers hardness was calculated from ten separate indentations.

$$HV = \frac{2P\ sin\frac{\theta}{2}}{D^2} \tag{3.4}$$

where P = load applied (kgf)

D = mean diagonal of the indentation (mm)

θ = angle between opposite faces of the diamond = 136°

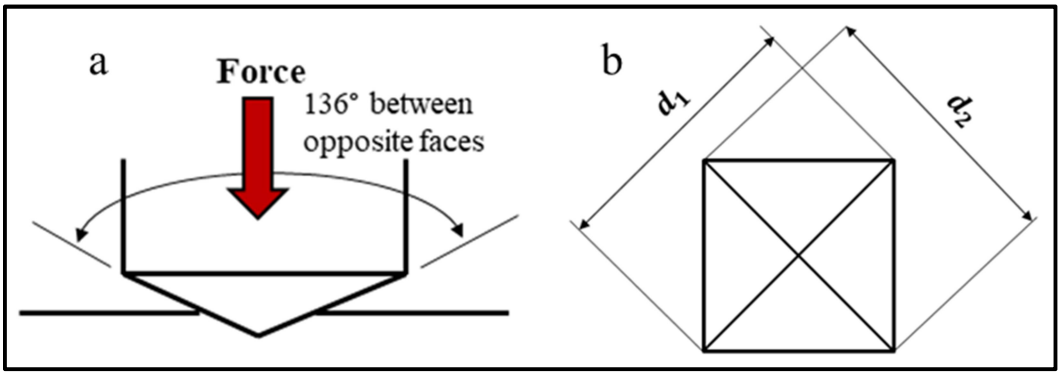

Fig. 3.5. (a) Schematic indentation marked by indenter, and (b) measurements of diagonal.

3.4.3 Compression test of the sintered HEAs

To assess the compressive strength of the sintered specimens, a compression test was performed using a universal testing machine (INSTRON 5982) in accordance with the ASTM E9-09 standard. The samples were shaped through wire electric discharge machining (EDM) from an initial sintered sample (diameter = ~15 mm and thickness = ~8 mm), resulting in dimensions of length (L) 8 mm and diameter (D) 4 mm, yielding an aspect ratio (L/D) of 2.0. The testing was performed at a controlled cross-head velocity of 0.1 mm/min under a load capacity of 40 kN. For consistency, two sets of samples underwent testing to ensure reproducibility. A pictorial image of the INSTRON universal testing machine during the compression test is shown in Fig. 3.6.

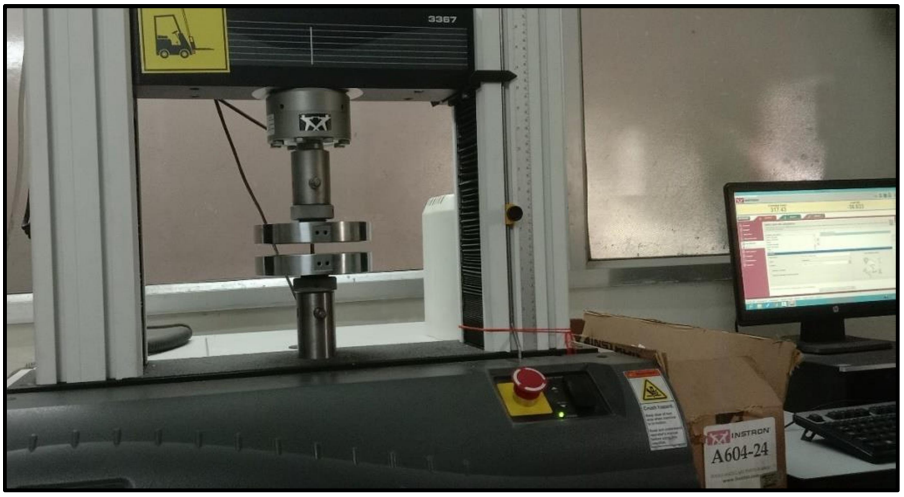

Fig. 3.6. Image of the INSTRON universal testing machine during the compression test.

3.5 Electrochemical corrosion measurements

The corrosion performance of the sintered samples (Ti-$Co_{0.35}$-$Cr_{0.35}$-Nb-Zr, Ti-Nb-Ta-Cr-$Co_{0.2}$, and Ti-Nb-Ta-$Fe_{0.35}$-$Co_{0.35}$ HEA) and Ti-6Al-4V alloy was tested in SBF with a pH of 7.4 at room temperature. Table 3.1 shows the composition of the SBF. The corrosion behaviour of the sintered samples was studied using electrochemical techniques, such as OCP, EIS, and PDP. Electrochemical measurements were conducted using a glass cell with a three-electrode system connected to a computer-controlled potentiostat (AUTOLAB, Netherlands). In the three-electrode system, the exposed surface (1 cm^2) of the sintered samples served as the working electrode. The system also included a saturated Ag/AgCl reference electrode and a graphite counter-electrode. The corrosion test set-up is shown in Fig. 3.7. OCP was conducted for 3600 s in SBF to stabilize the samples. Subsequently, EIS tests were performed with an A.C. amplitude range from −10 mV to +10 mV and a frequency range from 10^{-2} Hz to 10^{+5} Hz. The EIS data were analyzed through Nyquist and Bode-phase plots using the extrapolation method. Following this, PDP was measured with a scan rate of 1 mV per second. The corrosion parameters, such as corrosion potential (E_{corr}), and corrosion

current density (I_{corr}), were recorded from the polarization plots using Tafel analysis. To ensure repeatability, two parallel samples for each group were used. The surface after the corrosion tests was examined by FE-SEM.

Table 3.1 Chemical composition of simulated body fluid solution

Reagents	Amount in 1000 mL
NaCl	8.035
$NaHCO_3$	0.355
KCl	0.225
$K_2HPO_4.3H_2O$	0.231
$MgCl_2.6H_2O$	0.311
1.0 M HCl	39.0 ml
$CaCl_2$	0.292
Na_2SO_4	0.072
$((HOCH_2)_3CNH_2)$	6.118
1.0 M HCl	Appropriate amount to adjust pH to 7.4

Fig. 3.7. Corrosion test set-up.

3.6 Wear analysis of the sintered HEAs

The wear and friction assessment of sintered samples was carried out under wet conditions using an automated reciprocating friction monitor (TE 200ST) from Magnum Engineers, Bangalore, India. In the setup, the sintered samples (Ti-$Co_{0.35}$-$Cr_{0.35}$-Nb-Zr, Ti-Nb-Ta-Cr-$Co_{0.2}$ and Ti-Nb-Ta-$Fe_{0.35}$-$Co_{0.35}$ HEA) and Ti-6Al-4V alloy of diameter 15 mm and thickness 4 mm served as stationary bodies, while the counter material (ZrO_2 ball, ϕ10 mm) functioned as the moving body. The tests were conducted at a frequency of 2 Hz for 7200 cycles, covering a 3 mm sliding distance in the presence of SBF. A normal load of 10, 15, and 20 N was subjected to the counter material. To analyze the wear track, a contact profilometer (Taylor and Hobson in England) was used. The width and lateral depth of the wear track were quantified through the profilometer. Initially, the wear loss area of the worn profile was measured using the profilometer, and subsequently, average depth values were computed using a specified formula given by Eq. (3.5).

$$D_{avg} = \frac{A_w}{W} \tag{3.5}$$

Where, A_w, D_{avg}, and W denote the average wear loss area, average depth, and average width of each worn track, respectively. Finally, wear volume loss (ΔV) was calculated using the relation given by Eq. (3.6).

$$\Delta V = \left[\frac{1}{3} * \pi * D_{avg}^2\left(3R - D_{avg}\right)\right] + A_w * l \tag{3.6}$$

Where, l and R denote the length of the wear track and radius of the zirconia ball, respectively. The wear volume loss was converted into the wear rate (W_v) by using the relation given in Eq. (3.7).

$$W_v = \frac{\Delta V}{S} \tag{3.7}$$

Where, S defines the overall sliding distance. To ensure reproducibility, each experiment was conducted twice. FE-SEM (Nova Nano SEM 450) coupled with EDS, is used to observe the wear mechanism of the worn surfaces. The schematic representation of the linear motion reciprocating wear test is shown in Fig. 3.8.

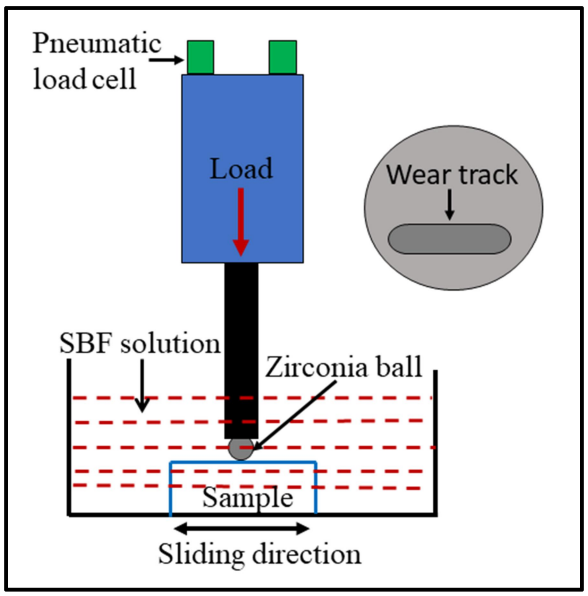

Fig. 3.8. Schematic representation of linear motion reciprocating wear test.

3.7 Cell culture

The biocompatibility assessment of the sintered specimens was conducted using MG-63 (human osteosarcoma) cells, which were obtained from NCCS Pune, Maharashtra, India. The culture medium used for this study consists of DMEM media (Dulbecco's modified eagle medium) with 15 % FBS and 1 % antibiotics. The cells (density = 10^4 cells/mL) were seeded onto the specimens placed in 24 well plates and subsequently placed in a standard incubation environment (37 °C, 95 % relative humidity, and 5 % CO_2) to facilitate cell growth. The cellular response was quantitatively assessed using the MTT [3-(4,5-dimethylthiazol-2-yl)-

2,5-diphenyl-2H-tetrazolium bromide] assay and qualitatively through fluorescence microscopy. A change of the DMEM medium was made every 48 or 72 h.

Cell proliferation was analyzed after 2, 4, and 6 days after seeding the cells over the sintered pellets. After the selected period of incubation, the media was removed and then it was rinsed twice with PBS solution. Afterward, 500 µL of reconstituted MTT was added to each well and incubated for 6 h. This facilitated the interaction between reconstituted MTT and viable cells, generating formazan crystals. After 6 h, dimethyl sulfoxide (DMSO) was introduced to the MTT solution in each well, followed by 10 min incubation under the same conditions to dissolve the formazan crystals. The quantity of these formazan crystals corresponded to the viability of live cells. To quantify this viability, an ELISA Microplate reader (iMark Bio-Red) was used to measure the optical density at 595 nm. The viability % of the sintered HEAs is calculated using the relation given in Eq. (3.8) [203].

$$Viability\ \% = \frac{OD_{sample}}{OD_{cp-T}}\ X\ 100\ \% \tag{3.8}$$

Where, $(OD)_{sample}$ means the OD value of the HEAs. Fluorescence microscopy was employed to investigate the adhesion and morphological changes of MG-63 cells upon contact with the sintered specimen. After 2, 4, and 6 days of the incubation period, the adhered cells were fixed using 4 % paraformaldehyde for 30 min at 4 °C. Subsequently, the cells underwent permeabilization with 0.1 % Triton X-100 for 10 minutes at room temperature. Now, bovine serum albumin was added to block these permeable cells. Staining was accomplished using Alexafluor 488 Phalloidin for the cytoskeleton and DAPI dyes for the nucleus of MG-63 cells. Imaging of these cells was performed using a fluorescent microscope (Nikon Eclipse LV 100 ND).